18

Indoor Positioning System Based on PSD Sensor

David Rodríguez-Navarro, José Luis Lázaro-Galilea, Alfredo Gardel-Vicente, Ignacio Bravo-Muñoz, Álvaro De-La-Llana-Calvo

DEPARTMENT OF ELECTRONICS, UNIVERSITY OF ALCALÁ, MADRID, SPAIN

1 Introduction

The chapter presents an indoor positioning system (IPS) based on the determination of the signal angle of arrival (AoA). It is focused in the use of infrared and luminous signals for positioning. This type of technology is possibly the least developed or used to date. The main reason is the lack of commercial sensors focused for positioning. Typically, the measurement methods for light sensor systems are based on point-to-point telemetry as is the case of LIDAR applications (light detection and ranging) (Kashani et al., 2015).

One of the most referenced works using this kind of technology for indoor applications is the so-called *the Active Badge System* (Want et al., 1992), which was implemented in a hospital where several staff people carried a device that emitted coded infrared signals. The positioning method was based on Cell-ID, a system which determines the room where each staff member was in.

AoA and time difference of arrival (TDoA) are two techniques widely used in obtaining agents position. The AoA technique is based on determining the AoA of the signal from the emitter to one or more receivers (if the geometry of the system is known, a single emitter would be enough).

An example of the use of AoA is presented in Lee et al. (2004), is based on three receivers composed of two photodiodes each, located in such a way that the mobile agent is enclosed within a small triangular coverage area. It is possible to measure the AoA differences between pairs of receivers and using an iterative method that minimizes a cost function, the position of the mobile agent is then obtained. As a disadvantage, the coverage of this positioning system (Lee et al., 2004) is limited to the overlapped area seen from the three receivers, which is only 40 cm wide.

On the other hand, TDoA technique is based on determining the difference time of arrival of the signal from an emitter to several receivers, using one of them as a reference, this time difference is proportional to distance differences and using multilateration

Geographical and Fingerprinting Data for Positioning and Navigation Systems. https://doi.org/10.1016/B978-0-12-813189-3.00018-6

algorithm the 3D position of the mobile agent is determined. This method requires four or more receivers. Examples of work jobs that use TDoA and optical signals are Gorostiza et al. (2011) and Salido-Monzú et al. (2014). The biggest handicap of the TDoA method is the multipath (MP) effect, as well as the synchronization in the acquisition of the signals captured from the different sensors. The accuracy obtained using simultaneous analogical-digital converters with the same reference clock is in the range of centimeters.

Concerning other potential functions of light-emitting diode (LED) light in the context of visible light communication (VLC) can be wireless communication and positioning, which make them an attractive research topic. The duplicate use of LEDs for lighting eliminates the cost of installing a positioning system based on VLC. Furthermore, the absence of electromagnetic interferences makes the use of LEDs particularly interesting; positioning based on VLC can be used as an indoor navigation system for location tracking, finding objects, controlling the movement of agents, etc.

Interesting works for the reader such as Huynh and Yoo (2016) propose a design for an IPS using LEDs, an image sensor (IS), and an accelerometer from mobile devices. The proposed scheme consists of four LEDs mounted on the ceiling transmitting their own 3D world coordinates and an IS at an unknown position receiving and demodulating the signals. Based on the 3D world coordinates and the 2D image coordinate of LEDs, the position of the mobile device is determined. To further improve accuracy, we propose a mechanism to reduce the IS noise. With the assumption that the IS coordinate space is parallel to the world reference plane, they evaluate the accuracy obtaining values below 10 cm. They also make a comparison with other state-of-the-art techniques such as Yoshino et al. (2008) and Nakazawa et al. (2013) showing the reaching of similar accuracy results.

Another example is presented in Xu et al. (2016), in which a visible light-based IPS was designed using multiple photodiodes in the environment and the received signal strength to determine the position of the mobile agent, obtaining mean error of 7 cm in a range of 2 m. The main problem encountered was the low signal-noise ratio as distance and angles increase. Work in Lin et al. (2017) proposes an indoor VLC and positioning system using the orthogonal frequency division multiplexing access scheme, in which the signals transmitted by LEDs are encoded with allocated subcarrier, respectively, and the receiver recovers all transmitted signals using a discrete Fourier transformation operation. The feasibility of the scheme is demonstrated in a room of size $20 \times 20 \times 15\,\text{cm}^3$. They show that the proposed scheme offers a mean positioning error of 1.68 cm, overcoming 2 cm of maximum error.

In another similar work (Kumaki et al., 2016), the authors also use four LEDs and IR camera. The paper proposes a fast coding/decoding scheme to be able to use low-cost artificial vision devices (e.g., smartphones). The research work (Sakai et al., 2016) proposes a different system, based on infrared light-emitting diode (IRED) beacons from the mobile agents and deploying an array of photodiodes as detectors. The 3D positioning is obtained by measuring the angle between the emitter and several photodiode receivers. The tests were done in a coverage area of $7 \times 2\,\text{m}^2$ obtaining errors up to 0.7 m.

The main drawback of these technologies concerns the MP by which the signal reaches the receivers. Looking solely at optical signals, the model of near-infrared signal reflection reported in De-La-Llana-Calvo et al. (2017) enabled us to model and analyze how this affects AoA and difference phase of arrival measurement techniques and take this into account in this study.

Concerning position sensitive device (PSD)-based systems, there are a few and also old research works for the indoor positioning of mobile agents, for example, Park et al. (2006) and Salomon et al. (2006). In Park et al. (2006), the authors propose a PSD-based IPS placed on a height of 2.5 m from floor to ceiling, making use of a Kalman filter to track a mobile robot that moves at a constant speed on a ground floor. The location results give a maximum error of 8.97 cm and average error of 1.97 cm, in a coverage area of 3×3 m^2. The maximum error comes from the location of the robot in the periphery of the monitored area.

On the other hand, (Salomon et al., 2006) propose a multiple PSD system located around the surveillance area where a mobile robot with an emitter moves freely. The positioning algorithm is done by means of trilateration, obtaining the distances from each PSD sensor and the robot through stereoscopic measurements. The results achieved in the test indicate that the error in the distance measurements increases linearly from 70 to 440 cm showing a nonlinear behavior outside of that distance boundary.

In the chapter, an IPS is described. The IPS accurately determines the position of mobile agents based on optical signals, using IREDs or LEDs emitters and a PSD sensor. The computational load of the system and measurement methods proposed is very low, making it possible to obtain a very high position update rate. We present in the chapter two different proposals for IPS with their corresponding evaluation. Section 2 describes the use of a PSD sensor and the mathematical model in a IPS. Section 3 is devoted to propose the calibration of the PSD sensor. Section 4 describes two different positioning methods. The last section summarizes the main conclusions of using this type of IPS.

2 Description and Modeling of the Optical Sensor System

We present an IPS for detecting mobile agents based on a single PSD sensor. The main goal is to develop an alternative IPS to other sensing technologies, cheaper, easier to install, and with a low computational load to obtain a high rate of measurements per second. The proposed IPS has the capacity to accurately determine 3D position from the AoA of the signal received at the PSD sensor.

The simplified receiver system, consisting of a PSD sensor and lens coupled, is shown in Fig. 1, where coordinate (x, y) represents the image of the (X, Y, Z) point on PSD sensor surface, (C_x, C_y) is the optical center, f is the focal length, (θ_x, θ_y) are the angular components of AoA, and (X, Y, Z) are the coordinates where the LED is located.

From the diagram given in Fig. 1 one can see that to compute the AoA we need to know the focal length value, center of projection, and the point of impact. Fig. 1 is a

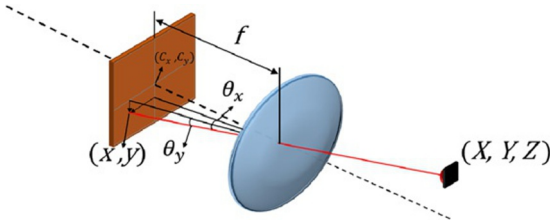

FIG. 1 Receiver based on position sensitive device sensor and lens coupled.

simplified representation, pinhole projection. In fact, the point of impact will be affected by distortions of the lenses, distortions of the PSD sensor, and misalignment of the ideal coupling of PSD and lens. Therefore, the optical center will not be in the center of the PSD sensor. So, in order to measure AoA with good accuracy, it is necessary to perform a previous calibration of the sensor (PSD + lens) system to correct these distortions. In other words, this calibration will obtain the values of the distortion parameters and the parameters involved in the determination of the impact point, such as the optical center and focal length.

2.1 PSD Sensor

Fig. 2 shows the equivalent electrical circuit of a 2D pincushion type for the PSD sensor. As we can see, PSD sensors have a common cathode and four anodes. The output current intensity for each anode will be inversely proportional to the distance between the point of impact of beam light and the position of the anode.

The impact point on the PSD surface is determined from the difference of the output currents in the four anodes, considering the origin of coordinates the center of the PSD sensor. Eqs. (1), (2) are used to calculate the impact point coordinates (x, y):

$$x = \frac{L_X}{2} \frac{(I_{X2} + I_{Y1}) - (I_{X1} + I_{Y2})}{I_{X1} + I_{X2} + I_{Y1} + I_{Y2}} \tag{1}$$

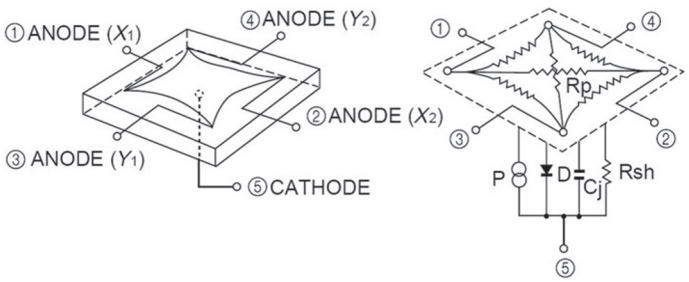

FIG. 2 Equivalent circuit of the PSD sensor pincushion. *(Courtesy of Hamamatsu.)*

$$y = \frac{L_Y}{2} \frac{(I_{X2} + I_{Y2}) - (I_{X1} + I_{Y1})}{I_{X1} + I_{X2} + I_{Y1} + I_{Y2}} \tag{2}$$

where I_{X1}, I_{X2}, I_{Y1}, and I_{Y2} are the output currents from the PSD sensor anode pins and L_X and L_Y are the sensor dimensions.

As will be discussed in the following section, it is not possible to calculate the point of incidence with these expressions because the PSD sensor output currents are very small and must be conditioned for digitization.

2.2 Electrical System Modeling

Due to the small value for the output currents of the PSD sensor, it is convenient to amplify them, first. Therefore, an amplification stage for each channel of the PSD sensor is included for further digitization. These stages will introduce some unbalances, noise, and quantification noise factors to the acquisition system. A typical electrical circuit model used, including the amplification stage, is shown in Fig. 3.

Eqs. (3), (4) will be used for calculating the impact point considering the amplifier's output voltage.

$$x = \frac{L_X}{2} \frac{(V_{X2} + V_{Y1}) - (V_{X1} + V_{Y2})}{V_{X1} + V_{X2} + V_{Y1} + V_{Y2}} \tag{3}$$

$$y = \frac{L_Y}{2} \frac{(V_{X2} + V_{Y2}) - (V_{X1} + V_{Y1})}{V_{X1} + V_{X2} + V_{Y1} + V_{Y2}} \tag{4}$$

In Eqs. (3), (4), $V_{\{X1,X2,Y1,Y2\}}$ are equal to $I_{\{X1,X2,Y1,Y2\}} \cdot K_{\{X1,X2,Y1,Y2\}}$, where $K_{\{X1,X2,Y1,Y2\}}$ are the gain factors of the amplification stages of each output channel of the PSD sensor.

Since these gain factors have a slightly different value for each channel, the calculation of the impact point will be affected. To mitigate this effect, it is proposed to add to the impact point equations a polynomial function, which will be the relationship between the gain factor of a channel (e.g., $G_1 = 1$ if it is used as a reference) and the other three.

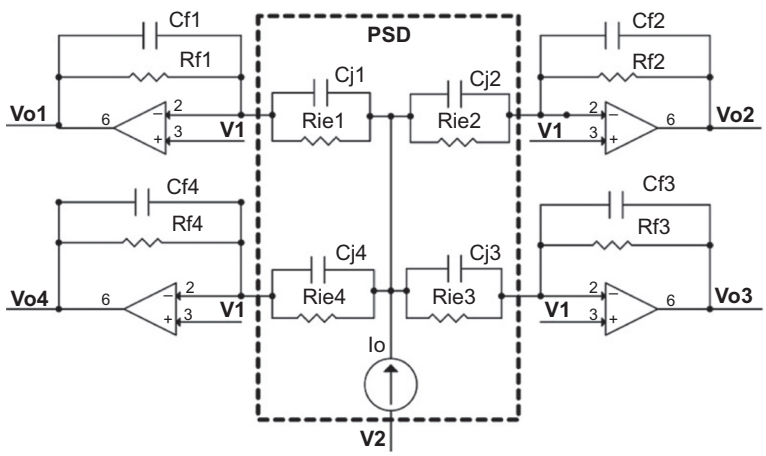

FIG. 3 Amplifier circuit from PSD sensor.

The difference between gain factors will be adjusted by a polynomial grade of order 2 (Eq. 5); however, in several cases it may be sufficient to use a linear approximation depending on the components used.

$$G_j = g_{1j}f^2 + g_{2j}f + g_{3j} \tag{5}$$

where $j = \{1, 2, 3, 4\}$ is related with each amplification stage, g are the coefficients of the polynomial, and f represents the frequency.

The new equations for the impact point considering the before gain model are as follows:

$$x = \frac{L_X}{2}\frac{(V_{X2}G_2 + V_{Y1}G_3) - (V_{X1}G_1 + V_{Y2}G_4)}{V_{X1}G_1 + V_{X2}G_2 + V_{Y1}G_3 + V_{Y2}G_4} \tag{6}$$

$$y = \frac{L_Y}{2}\frac{(V_{X2}G_2 + V_{Y2}G_4) - (V_{X1}G_1 + V_{Y1}G_3)}{V_{X1}G_1 + V_{X2}G_2 + V_{Y1}G_3 + V_{Y2}G_4} \tag{7}$$

Section 3 describes the calibration procedures for obtaining parameters $g_{i,j}$.

2.3 Optical System Modeling

A simple pinhole model has been proposed for the optical system modeling. This is the most common perspective projection for an optical system, which relates the environment coordinates (3D) with the image formed in the PSD sensor plane (2D).

Fig. 4 represents the pinhole model, where (X_W, Y_W, Z_W) are the axes of the world reference system, (X_R, Y_R, Z_R) are the PSD sensor reference system axes, (x, y) is the impact point on the PSD sensor surface, f is the focal length, (C_x, C_y) is the optical center, R is the rotation matrix, and T is the translation vector which relates the different coordinate systems.

The relationship between the world reference system and the receiver reference system is related to the 3×3 rotation matrix (R) and the 3×1 translation vector (T), according to Eq. (8).

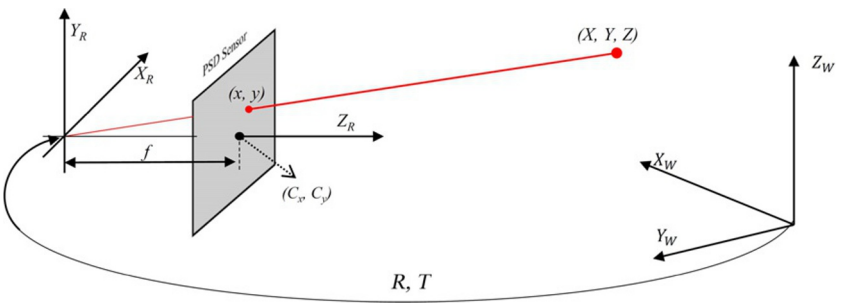

FIG. 4 Pinhole model.

$$\begin{pmatrix} X_R \\ Y_R \\ Z_R \end{pmatrix} = R \begin{pmatrix} X_W \\ Y_W \\ Z_W \end{pmatrix} + T \tag{8}$$

Next we show the relationship between the receiver's reference system and the image plane, Eq. (9) being the one that represents this relationship.

$$\begin{pmatrix} sx \\ sy \\ s \end{pmatrix} = \begin{pmatrix} f & 0 & C_x \\ 0 & f & C_y \\ 0 & 0 & 1 \end{pmatrix} \begin{pmatrix} X_R \\ Y_R \\ Z_R \end{pmatrix} \tag{9}$$

where s represents the scale factor that relates the 3D to 2D projection.

The matrix system (10) presents the mathematical model of the receiver, without taking into account the distortions produced by the lens and the PSD sensor.

$$\begin{pmatrix} sx \\ sy \\ s \end{pmatrix} = \underbrace{\begin{pmatrix} f & 0 & C_x \\ 0 & f & C_y \\ 0 & 0 & 1 \end{pmatrix}}_{A} \underbrace{\begin{pmatrix} r_{11} & r_{12} & r_{13} & T_x \\ r_{21} & r_{22} & r_{23} & T_y \\ r_{31} & r_{32} & r_{33} & T_z \end{pmatrix}}_{RT} \begin{pmatrix} X_W \\ Y_W \\ Z_W \\ 1 \end{pmatrix} \tag{10}$$

The elements of matrix A together with the parameters that model the distortions, which will be shown below, are called intrinsic parameters, since they depend solely on the configuration of the sensor (PSD + lens), regardless of its position and orientation in the world reference system.

Additionally, the RT matrix contains the extrinsic parameters, since they depend on the position and orientation between the two reference systems independently of the sensor configuration used.

As mentioned above, this is a linear model and therefore does not take into account the lens distortion or sensor distortion; therefore, it is necessary to add nonlinear effects caused by the lens and PSD sensor. Due to the low distortion produced by pincushion sensors, it will be the distortion of the lens that predominates, so only this factor will be included in the model.

Typically, the distortion of lenses is modeled taking into account two different effects: radial and tangential distortions. Beginning with radial distortion, Eqs. (11), (12) model this type of distortion.

$$D_x^r = (x^d - C_x)(a_1 r^2 + a_2 r^4 + \cdots + a_n r^{2n}) \tag{11}$$

$$D_y^r = (y^d - C_y)(a_1 r^2 + a_2 r^4 + \cdots + a_n r^{2n}) \tag{12}$$

where r is the Euclidean distance from the distorted point (x^d, y^d) to the optical center (C_x, C_y), and $a_{\{1,2,\ldots,n\}}$ are the parameters that model the radial distortion of the lenses.

In the case of tangential distortion, this is modeled according to Eqs. (13), (14).

$$D_x^t = p_1 \left(r^2 + 2\left(x^d - C_x\right)^2 \right) + 2p_2 \left(x^d - C_x\right)\left(y^d - C_y\right) \tag{13}$$

$$D_y^t = p_2\left(r^2 + 2\left(y^d - C_y\right)^2\right) + 2p_1\left(x^d - C_x\right)\left(y^d - C_y\right) \tag{14}$$

where p_1 and p_2 represent the parameters that model the tangential distortion of the lens.

Therefore, by adding the distortion parameters to the linear model, we obtain Eqs. (15), (16), being (x, y) the impact point considering that there is no distortion.

$$x^d = x + D_x^r + D_x^t \tag{15}$$

$$y^d = y + D_y^r + D_y^t \tag{16}$$

To retrieve the AoA and impact point we require the use of all the parameters considered in the sensor system model. Next section describes the calibration of the sensor system to obtain the parameter values of the given sensor system model.

3 Sensor System Calibration

As mentioned, it is necessary to calibrate the system in order to make precise measurements. The calibration process is based on two stages: first, an electrical calibration and then, a geometric calibration.

3.1 Electrical Calibration Process

In previous section, it has been introduced that electrical circuit for signal conditioning adds errors in the impact point determination; the most common error factors are differences in channels gain, noise, and quantification noise factors. In Rodríguez-Navarro et al. (2016) each one of these factors is analyzed, concluding that the system noise introduces random errors that can be reduced using digital band-pass filters, while the gain differences are systematic errors that can be corrected following the process indicated below.

To correct gain factor misadjustments, an electrical calibration must be carried out. This calibration is based on a uniform illumination of the PSD sensor whole area. The uniform illumination should give the same value for the PSD sensor output currents. So, any difference will be considered an unbalanced amplifiers gain.

To illuminate the PSD sensor uniformly, it is recommended to use a IRED with the widest radiation pattern possible placed in front of the PSD sensor at a distance that makes the solid angle less than 0.01 Sr. Considering a squared sensor with a radius of 10 mm, the emitter should be located at a minimum distance equal to $d = \sqrt{\frac{10 \cdot 10^{-3}}{0{\cdot}01}} = 1$ m. This scenario ensures uniform illumination throughout the PSD sensor (Fig. 5).

The root mean square (RMS) values of the signals are compared with the reference signal value, obtaining the relationship between the reference and the other signals. This should be adjusted or modeled for the entire working frequency range of the modulated emitted signal. If a single frequency is used, the ratio is a constant; if the IPS will be used for

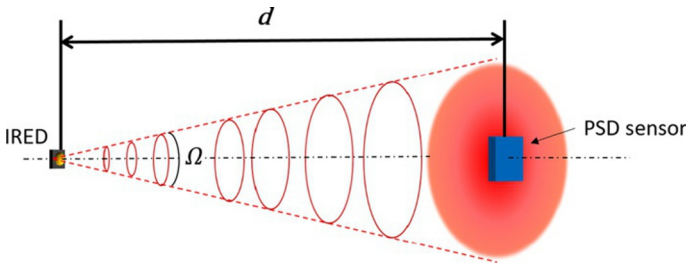

FIG. 5 Uniform illumination of the PSD sensor.

different signal frequencies, an expression of the variation of the gain factor as a function of frequency should be obtained.

Once the RMS values of each signal for a frequency range have been obtained, the coefficients of the polynomial equation (5) for least squares error minimization are calculated, using the equation $Ax = b$. The standard solution that minimizes this equation is $x = (A'A)^{-1}A'b$, where

$$A = \begin{pmatrix} \mathbf{F}^2 & \mathbf{F} & 1 \end{pmatrix}$$

$$x = \begin{pmatrix} a_{11} & a_{12} & a_{13} & a_{14} \\ a_{21} & a_{22} & a_{23} & a_{24} \\ a_{31} & a_{32} & a_{33} & a_{34} \end{pmatrix}$$

$$b = \begin{pmatrix} \frac{\mathbf{V_{ref}}}{\mathbf{V_1}} & \frac{\mathbf{V_{ref}}}{\mathbf{V_2}} & \frac{\mathbf{V_{ref}}}{\mathbf{V_3}} & \frac{\mathbf{V_{ref}}}{\mathbf{V_4}} \end{pmatrix}$$

where $\mathbf{F}$ is a column vector with those frequencies at which the RMS values have been calculated, $\mathbf{V_{ref}}$ the column vector with the RMS values of the reference signal, $\mathbf{V}_{\{1,2,3,4\}}$ the column vectors with the RMS values of the sensor output channels and the matrix x containing the coefficients of the fitting polynomials.

Once the channel imbalances have been compensated, next stage is geometrical calibration. If the gain factors are unbalanced, it is important to perform an electrical calibration beforehand, because errors at the impact point will affect the geometric calibration critically.

3.2 Geometric Calibration

The objective of this stage is to calculate the optical system parameter values, using non-linear system algorithms (Fletcher, 2013) (Gauss-Newton, Levenberg-Marquardt, gradient descent, etc.). One problem associated with these techniques is that they may converge on a solution that is mathematically correct, but that does not conform to reality. In order to avoid this situation, it is necessary to establish a good starting point, based on

an approximate knowledge of the real parameter values or obtaining an approximation analytically.

The flow diagram for geometric calibration of the system is shown in Fig. 6. This process has been subdivided into four steps, which are acquisition of images, calculation of the projection matrix, extraction of intrinsic and extrinsic parameters, and iterative method to obtain distortion parameters.

- *Image acquisition.* The acquisition of images refers to the acquisition of impact points from a set of IREDs placed in a 2D pattern. Fig. 7 shows an example of a 2D IRED pattern, in which the coordinates of these points are known. The minimum requirement for the calibration procedure is that the calibration pattern has at least five points and takes three images for the whole pattern in different locations. However, it is advisable to have a pattern with 15–20 points and take between 8 and 12 images, depending on the noise in the system and the lenses distortion.

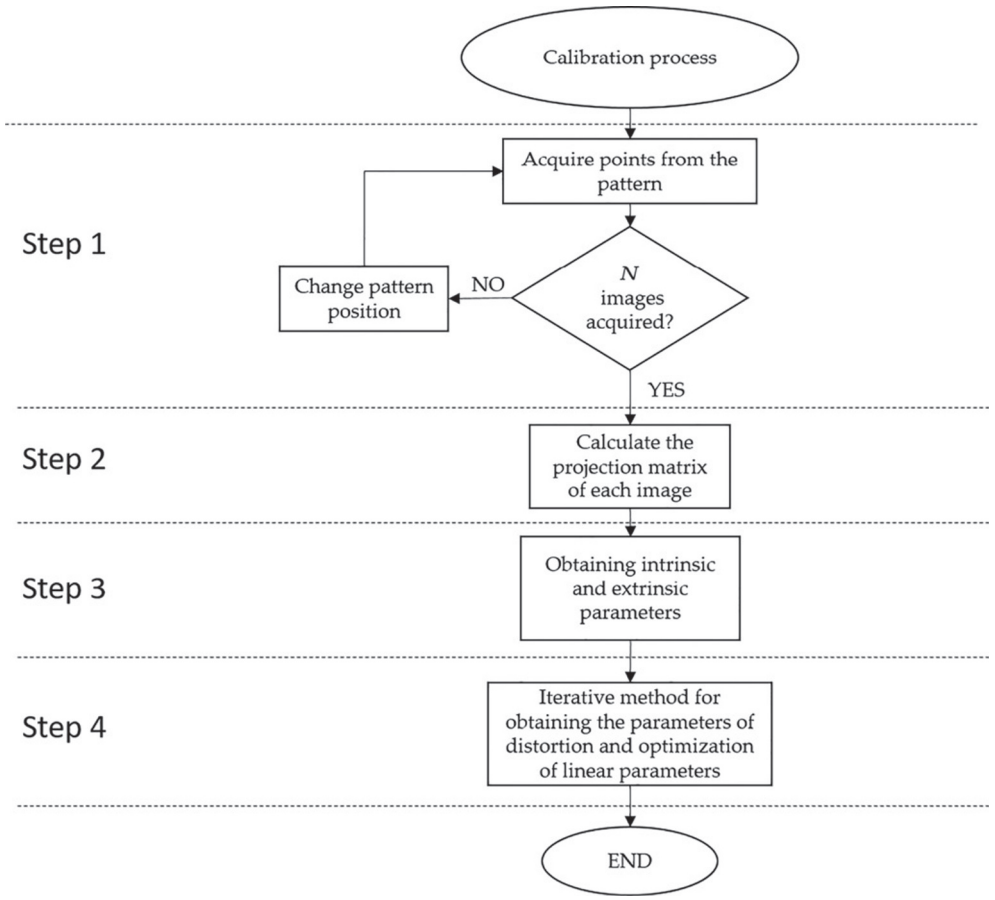

FIG. 6 The flow diagram for geometric calibration of the system.

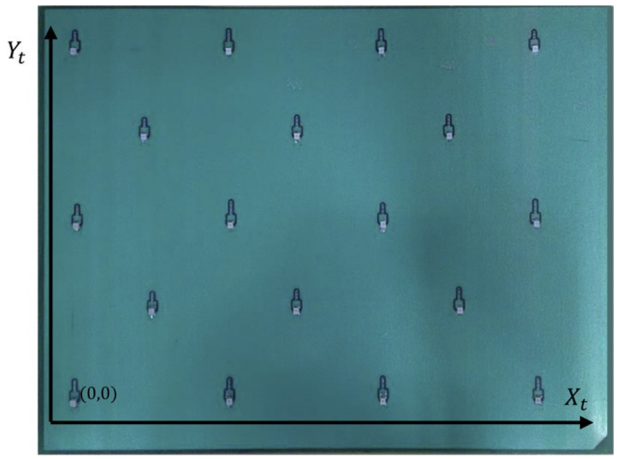

FIG. 7 Example of a calibration pattern including 18 IREDs.

- *Projection matrix for each captured image.* Once all images have been captured, it is necessary to obtain the corresponding projection matrix for each one. Starting from Eq. (17) that relates the pattern points with the impact points captured in the sensor.

$$\begin{pmatrix} sx \\ sy \\ s \end{pmatrix} = M \begin{pmatrix} X_t \\ Y_t \\ 1 \end{pmatrix} = \begin{pmatrix} m_{11} & m_{12} & m_{13} \\ m_{21} & m_{22} & m_{23} \\ m_{31} & m_{32} & m_{33} \end{pmatrix} \begin{pmatrix} X_t \\ Y_t \\ 1 \end{pmatrix} \tag{17}$$

where (x, y) are the coordinates of the impact point in the sensor, M is a 3×3 homography and (X_t, Y_t) the coordinates of corresponding point in the calibration template. By means of Eq. (17), from each image we can obtain 2 equations like those shown in Eqs. (18 and 19).

$$m_{11}X'_t + m_{12}Y'_t + m_{13} - m_{31}X'_t x' - m_{32}Y'_t x' - m_{33}x' = 0 \tag{18}$$

$$m_{21}X'_t + m_{22}Y'_t + m_{23} - m_{31}X'_t y' - m_{32}Y'_t y' - m_{33}y' = 0 \tag{19}$$

where (X'_t, Y'_t) are the column vectors of the coordinates of the 2D IRED locations in the calibration pattern and (x', y') are the column vectors of the projection on the sensor of the impact points of the corresponding IREDs. In matrix form it can be expressed as:

$$\begin{pmatrix} X'_t & Y'_t & 1 & 0 & 0 & 0 & -x'X'_t & -x'Y'_t - x' \\ 0 & 0 & 0 & X'_t & Y'_t & 1 & -y'X_t & -y'Y'_t - y' \end{pmatrix} \begin{pmatrix} m_{11} \\ m_{12} \\ \vdots \\ m_{33} \end{pmatrix} = 0 \tag{20}$$

This expression is solved by singular-value decomposition (SVD), thus obtaining the projection matrix.

- *Obtaining intrinsic and extrinsic parameters.* The projection matrix is composed of intrinsic parameters (A) multiplied by the extrinsic parameters matrix $\begin{pmatrix} r_1 & r_2 & t \end{pmatrix}$ as shown in Eq. (21).

$$\begin{pmatrix} sx \\ sy \\ s \end{pmatrix} = M \begin{pmatrix} X_t \\ Y_t \\ 1 \end{pmatrix} = A \begin{pmatrix} r_1 & r_2 & t \end{pmatrix} \begin{pmatrix} X_t \\ Y_t \\ 1 \end{pmatrix} \tag{21}$$

Knowing that $[m_1 \quad m_2 \quad m_3] = A[r_1 \quad r_2 \quad t]$, where m_i are the columns of matrix M, A is the matrix containing the intrinsic parameters, r_i are the columns of the rotation matrix, and t is the translation vector, we know that since the rotation matrix is orthonormal, the following relationships can be applied: $r_1^T r_2 = 0$ and $r_1^T r_1 = r_2^T r_2$. Consequently, from these constraints, we obtain Eqs. (22), (23).

$$m_1^T A^{-T} A^{-1} m_2 = 0 \tag{22}$$

$$m_1^T A^{-T} A^{-1} m_2 = 0 \tag{23}$$

where $A^{-T}A^{-1}$ results in the matrix B given in Eq. (24), which is the proposal for our model, where the focal length parameter is considered of equal value for the two coordinate axes.

$$B = A^{-T}A^{-1} = \begin{pmatrix} \frac{1}{f^2} & 0 & \frac{-C_x}{f^2} \\ 0 & \frac{1}{f^2} & \frac{-C_y}{f^2} \\ \frac{-C_x}{f^2} & \frac{-C_y}{f^2} & \frac{-C_x^2}{f^2} + \frac{-C_y^2}{f^2} + 1 \end{pmatrix} = \begin{pmatrix} b_{11} & b_{12} & b_{13} \\ b_{21} & b_{22} & b_{23} \\ b_{31} & b_{32} & b_{33} \end{pmatrix} \tag{24}$$

As the matrix B is symmetrical, it is only necessary to obtain six elements, so the vector is $b = [\ b_{11} \quad b_{12} \quad b_{22} \quad b_{13} \quad b_{23} \quad b_{33}\ ]^T$. The elements of matrix B are traditionally obtained using Eq. (25), where
$V_{ij} = [m_{i1}m_{j1} \ \ m_{i1}m_{j2} + m_{i2}m_{j1} \ \ m_{i2}m_{j2} \ \ m_{i3}m_{j1} + m_{i1}m_{j3} \ \ m_{i3}m_{j2} + m_{i2}m_{j3} \ \ m_{i3}m_{j3}]$,
where m_{ij} are the elements of the projection matrix obtained in previous step.

$$\begin{bmatrix} V_{12}^T \\ (V_{11} - V_{22})^T \end{bmatrix} b = 0 \tag{25}$$

Once the matrix system (25) has been solved and according to B matrix, the system's linear intrinsic parameters are obtained by means of the following equations:

$$C_x = -b_{11}/b_{13} \tag{26}$$

$$C_y = -b_{22}/b_{23} \tag{27}$$

$$f = \sqrt{1}/b_{11} \tag{28}$$

Then, the projection matrices for each image are used to calculate the extrinsic parameters as follows:

$$r_1 = \lambda A^{-1} m_1 \tag{29}$$

$$r_2 = \lambda A^{-1} m_2 \tag{30}$$

$$r_3 = r_1 \times r_2 \tag{31}$$

$$t = \lambda A^{-1} m_3 \tag{32}$$

where $\lambda = \left\| \frac{1}{A^{-1} m_1} \right\| = \left\| \frac{1}{A^{-1} m_2} \right\|$. Due to image noise and nonlinearity, these parameters contain error because we are using linear techniques to solve a nonlinear problem.

- *Iterative method.* Having obtained approximate linear parameter values, the extrinsic and intrinsic parameters that model the system are obtained/optimized, in our case using the Levenberg-Marquardt algorithm.
  The function to be minimized is the following:

$$f(x) = \sum_{i=1}^{n} \left\| Q_i - \hat{Q}_i(A, D, R_i, T_i, P) \right\|^2 \tag{33}$$

where n is the number of images, Q are the points in the image plane, A is the intrinsic matrix containing the parameters, such as the focal length and optical center, vector D contains the parameters that model distortion, R and T are the rotation matrix and the translation vector, respectively, P are the calibration template points, and $\hat{Q}$ are the points in the image plane obtained from the intrinsic and extrinsic parameters and the calibration template points.

Once all parameters have been computed, the distortion caused by the lens can be corrected and the AoA calculated. With the calibration performed, we proceed to describe the 3D positioning methods using AoA.

4 Three-Dimensional Position Determination Using AoA

This section describes two methods for determining the 3D position using only one sensor and AoA measurement, and possible error factors in the 3D measurement.

4.1 Method 1: IPS Located in the Environment and IRED on Board of the Mobile Agent

Fig. 8 shows the IPS consisting of the sensor located on the ceiling and the IREDs on the mobile agents. Assuming the plane in which agents are moving is known, it is possible to determine the 3D position of the *agent* by means of the intersection of the line given by the corresponding AoA and plane of movement.

In Fig. 8, (X, Y, Z) are the environment coordinates with reference to the origin of the receiver position and (A, B, C, D) are the parameters that model the plane.

The proposed method is based on the following three steps:

- compute the parameters of the movement plane (offline);
- obtain the AoAs; and
- determine the 3D position of each mobile agent by means of the intersection of the plane and the line given by each AoA.

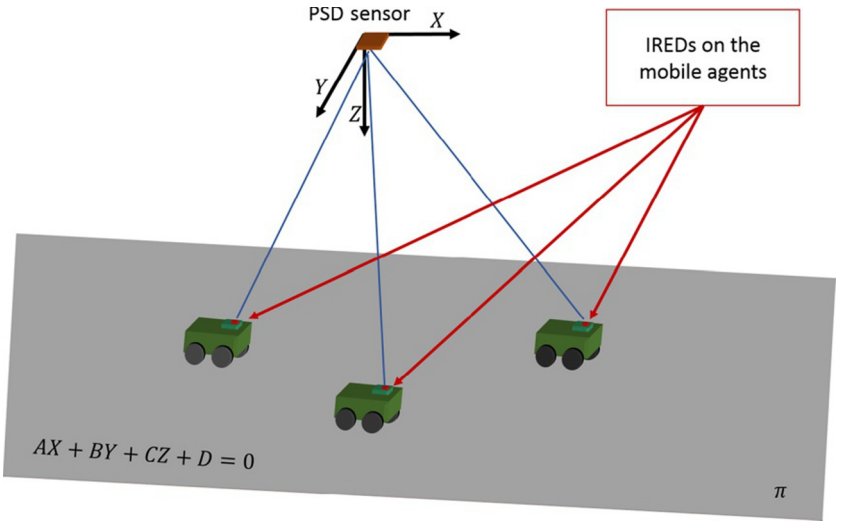

FIG. 8 IPS with receiver located in the environment and IREDs on mobile agents.

To compute the movement plane parameters is necessary to have at least four points belonging to the plane. Then, the plane equation parameters are directly obtained from an SVD procedure.

The 3D coordinates of those plane points are obtained by taking the image from four or more IREDs in different positions on the plane covering as much area as possible, and thus obtaining the rotation matrix and translation vector.

Therefore, the first step is to obtain the projection matrix, as it was previously described in Section 3 for the geometric calibration, using Eq. (20) considering now that (X_t', Y_t') are the coordinates of the points in the plane (taking one as the world reference system), and (x', y') are the corresponding impact point projections on the sensor with the distortion corrected, by means of the projection matrix M.

Since the intrinsic parameters (matrix A) and the elements of matrix M are already known from the geometric calibration, by means of Eqs. (29)–(32) the rotation matrix (R) and the translation vector (T), the extrinsic parameters for the movement plane are determined.

Finally, multiplying the (X_t', Y_t') points by the rotation matrix and adding the translation vector, the 3D coordinates for the points of the plane with reference to the sensor origin can be obtained.

Once the 3D points in the plane have been determined, the matrix equation to obtain the parameters of the plane is as follows:

$$(X' \; Y' \; Z') \begin{pmatrix} A \\ B \\ C \\ D \end{pmatrix} = 0 \tag{34}$$

where (X', Y', Z') are column vectors of the 3D coordinates for the plane points obtained earlier.

Once the plane equation and the intrinsic parameters are known, it is possible to obtain the angular components of each AoA using Eqs. (35), (36).

$$\theta_x = \tan^{-1} \frac{(x - C_x)}{f} \tag{35}$$

$$\theta_y = \tan^{-1} \frac{(y - C_y)}{f} \tag{36}$$

where (x, y) is the impact point with corrected distortion, (C_x, C_y) is the optical center, f is the focal length, and (θ_x, θ_y) are the angular components of AoA.

After computing the AoA values, the equation of straight line that goes from the corresponding emitter to the impact point in the PSD sensor can be obtained as:

$$X_i = \tan\theta_{xi} Z_i \tag{37}$$

$$Y_i = \tan\theta_{yi} Z_i \tag{38}$$

where i represents each mobile agent, and (X, Y, Z) are the 3D point coordinates refereed to the PSD sensor coordinate system.

Combining Eqs. (37), (38) with the plane equation we can obtain the Z coordinate of the line-plane intersection.

$$Z_i = -\frac{D}{A\tan\theta_{xi} + B\tan\theta_{yi} + C} \tag{39}$$

Therefore, replacing Z in Eqs. (37), (38) the 3D coordinate of the mobile agent with reference to the sensor reference system is obtained.

It is possible to change the reference coordinate system. It can be done by means of the matrix system (40), where (X_i, Y_i, Z_i) are the coordinates of each mobile agent, (X_i^p, Y_i^p, Z_i^p) are the 3D coordinates referred to the movement plane (where Z_i^p is null), R is the rotation matrix, and T is the translation vector for the point plane chosen as the origin of the world reference system.

$$\begin{pmatrix} X_i^p \\ Y_i^p \\ Z_i^p \end{pmatrix} = R \begin{pmatrix} X_i \\ Y_i \\ Z_i \end{pmatrix} + T \tag{40}$$

4.2 Method 2: PSD Sensor on Board of Each Mobile Agent and Emitters in the Environment

In this method the location of the PSD sensors and the emitters are exchanged; that is, the emitters are located in the ceiling of the environment and each mobile agent has its own PSD sensor. With this IPS configuration, the lighting infrastructure based on LEDs could also be used for positioning, resulting in a lower cost.

This type of IPS is shown in Fig. 9. In this case, assuming that the plane of movement is parallel to the ceiling; each PSD sensor (mobile agent) must receive a signal from three or more LEDs simultaneously in order to obtain an absolute positioning solution.

Considering the diagram given in Fig. 9, the position of a mobile agent (x, y) with respect to each of the emitters provides two equations given by Eqs. (41), (42).

$$x_i = \cos\beta_i \tan\theta_i h + P_{xi} \tag{41}$$

$$y_i = \sin\beta_i \tan\theta_i h + P_{yi} \tag{42}$$

where θ is the AoA, β is the angle of orientation, and (P_x, P_y, h) is the position of the LED considering the ceiling is at a height h and the LED is located in the point (P_x, P_y) respect the plane $x - y$, and i is the current mobile agent.

It is worth noting that system to be solved contains one variable (h) plus another one for each LED (β). In other words, in the case of three LEDs there would be four variables to be determined and six equations (positions of the emitters are known). However, depending on the locations of the LEDs it could happen that some equations are dependent and therefore there is more than one possible solution. This is the reason why we need at least three emitters.

Due to errors, intersections among beams from three or more emitters do not cross at a single point, so we use an optimization method for determining the 3D position of the mobile agent with the least error. Function to be minimized is given by Eq. (43).

$$\varepsilon(\beta_i, h) = \sum_{i=1}^{n-1} \sum_{j=1}^{n} (\Phi_i - \Phi_{i+j})^2 \tag{43}$$

where Φ represents Eqs. (41), (42).

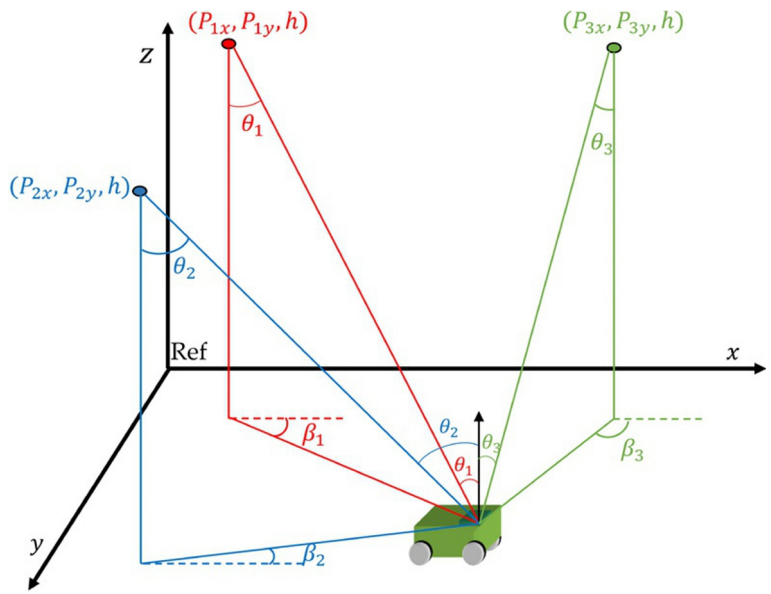

FIG. 9 IPS using LEDs for illuminating and receiver on mobile agent.

5 Discussion

Two proposals have been presented for indoor positioning; the first of them uses a single PSD sensor and a single IRED (or LED), but it is necessary to calibrate the plane of movement in order to be able to determine the intersection of the straight line given by the obtained AoA and the plane; the second method requires three LEDs and a PSD sensor on board each mobile agent, with the advantage that it is not necessary to calibrate the plane and that already installed lighting LEDs can be used.

Both methods are based on AoA measurements so that for a precise positioning it is necessary to calibrate the PSD sensor system. To do so, a procedure divided in two stages has been described: first the electrical calibration, which compensates any deviation in the signal conditioning stages, and second the geometric calibration where the values of the parameters that model the PSD sensor plus lens system are obtained also considering the distortion parameters to correctly determine the AoA.

In conclusion, when choosing an IPS system to locate an agent in a large area (e.g., a room inside a building) any of the existing alternatives can be used. However, when the position must be obtained with accuracy of centimeters at a high rate of measurements, suitable solutions are those using ultrasound and infrared. Infrared-based systems have the advantage that they are immune to electromagnetic noise and much less sensitive to MP effects, making them ideal for narrow spaces such as corridors.

Acknowledgments

This research was supported by the Spanish research program through the Indoor Positioning and Indoor Navigation Spanish Network (REPNIN) (TEC2015-71426-REDT) and through the ALCOR project (DPI2013-47347-C2-1-R).

References

De-La-Llana-Calvo, Á., Lázaro-Galilea, J.L., Gardel-Vicente, A., Rodríguez-Navarro, D., Bravo-Muñoz, I., Tsirigotis, G., Iglesias-Miguel, J., 2017. Modeling infrared signal reflections to characterize indoor multipath propagation. Sensors 17, 4. https://doi.org/10.3390/s17040847. Available from: http://www.mdpi.com/1424-8220/17/4/847.

Fletcher, R., 2013. Practical Methods of Optimization. John Wiley & Sons, New York, NY.

Gorostiza, E.M., Lázaro Galilea, J.L., Meca Meca, F.J., Salido Monzú, D., Espinosa Zapata, F., Pallarés Puerto, L., 2011. Infrared sensor system for mobilerobot positioning in intelligent spaces. Sensors 11 (5), 5416–5438. https://doi.org/10.3390/s110505416. Available from: http://www.mdpi.com/1424-8220/11/5/5416.

Huynh, P., Yoo, M., 2016. VLC-based positioning system for an indoor environment using an image sensor and an accelerometer sensor. Sensors 16 (6). https://doi.org/10.3390/s16060783. Available from: http://www.mdpi.com/1424-8220/16/6/783.

Kashani, A.G., Olsen, M.J., Parrish, C.E., Wilson, N., 2015. A review of LIDAR radiometric processing: from ad hoc intensity correction to rigorous radiometric calibration. Sensors 15 (11), 28099–28128. https://doi.org/10.3390/s151128099. Available from: http://www.mdpi.com/1424-8220/15/11/28099.

Kumaki, H., Akiyama, T., Hashizume, H., Sugimoto, M., 2016. 3D indoor positioning and rapid data transfer using modulated illumination. In: Proceedings of the International Conference on Indoor Positioning and Indoor Navigation (IPIN). Alcalá de Henares, Spain, pp. 4–7.

Lee, C., Chang, Y., Park, G., Ryu, J., Jeong, S.-G., Park, S., Park, J.W., Lee, H.C., Shik Hong, K., Lee, M.H., 2004. Indoor positioning system based on incident angles of infrared emitters. In: 30th Annual Conference of IEEE Industrial Electronics Society, 2004. IECON 2004, vol. 3, pp. 2218–2222.

Lin, B., Tang, X., Ghassemlooy, Z., Lin, C., Li, Y., 2017. Experimental demonstration of an indoor VLC positioning system based on OFDMA. IEEE Photonics J. 9 (2), 1–9. https://doi.org/10.1109/JPHOT.2017.2672038.

Nakazawa, Y., Makino, H., Nishimori, K., Wakatsuki, D., Komagata, H., 2013. Indoor positioning using a high-speed, fish-eye lens-equipped camera in visible light communication. In: International Conference on Indoor Positioning and Indoor Navigation, pp. 1–8.

Park, J.-H., Won, D.-H., Park, K.-Y., Baeg, S.-H., Baeg, M.-H., 2006. Development of a real time locating system using PSD under indoor environments. In: 2006 SICE-ICASE International Joint Conference, pp. 4251–4255.

Rodríguez-Navarro, D., Lázaro-Galilea, J.L., Bravo-Muñoz, I., Gardel-Vicente, A., Tsirigotis, G., 2016. Analysis and calibration of sources of electronic 460 error in PSD sensor response. Sensors 16 (5). https://doi.org/10.3390/s16050619. Available from: http://www.mdpi.com/1424-8220/16/5/619.

Sakai, N., Zempo, K., Mizutani, K., Wakatsuki, N., 2016. Linear positioning system based on IR beacon and angular detection photodiode array. In: Proceedings of the International Conference on Indoor Positioning and Indoor Navigation (IPIN). Alcalá de Henares, Spain, pp. 4–7.

Salido-Monzú, D., Martín-Gorostiza, E., Lázaro-Galilea, J.L., Martos-Naya, E., Wieser, A., 2014. Delay tracking of spread-spectrum signals for indoor optical ranging. Sensors 14 (12), 23176–23204. https://doi.org/10.3390/s141223176. Available from: http://www.mdpi.com/1424-8220/14/12/23176.

Salomon, R., Schneider, M., Wehden, D., 2006. Low-cost optical indoor localization system for mobile objects without image processing. In: 2006 IEEE Conference on Emerging Technologies and Factory Automation, pp. 629–632.

Want, R., Hopper, A., Falcão, V., Gibbons, J., 1992. The active badge location system. ACM Trans. Inf. Syst. 10 (1), 91–102. https://doi.org/10.1145/128756.128759.

Xu, Y., Zhao, J., Shi, J., Chi, N., 2016. Reversed three-dimensional visible light indoor positioning utilizing annular receivers with multi-photodiodes. Sensors 16 (8), 1254. https://doi.org/10.3390/s16081254. Available from: http://www.mdpi.com/1424-8220/16/8/1254.

Yoshino, M., Haruyama, S., Nakagawa, M., 2008. High-accuracy positioning system using visible LED lights and image sensor. In: 2008 IEEE Radio and Wireless Symposium, pp. 439–442.